Full Determination of Zero Field Splitting Tensor of the Excited Triplet State of C_{60} Derivatives of Arbitrary Symmetry from High Field TREPR in Liquid Crystals

Marco Bortolus,[†] Alberta Ferrarini,[†] Johan van Tol,[‡] and Anna Lisa Maniero*[,†]

Dipartimento di Scienze Chimiche, Università di Padova, Via Marzolo 1, I-35131 Padova, Italy, and CIMAR, National High Magnetic Field Laboratory, Florida State University, Tallahassee, Florida 32306

Received: October 28, 2005; In Final Form: November 30, 2005

The low-lying photoexcited triplet state of a series of fullerene C_{60} adducts has been studied by high-field TREPR (time-resolved EPR) spectroscopy in a partially oriented phase. The fullerenes adopt a biaxial alignment, driven by the substituents, that has allowed to fully determine the **ZFS** and **g** tensors, i.e., their principal values and the orientation of the principal axes in the molecular skeleton. This has been accomplished by combining line shape analysis and theoretical prediction of molecular order. A strong dependence of the magnetic tensors on the substitution pattern has been found.

Introduction

Fullerenes show unique photophysical properties that are mostly retained by their derivatives. They are good optical limiters and excellent electron and energy acceptors, both in the ground and excited states.[1] These properties make them suitable building blocks for electrooptical devices or artificial reaction centers.[2,3] In many fullerenes, the low-lying triplet state is formed with high efficiency, following light absorption, and exhibits long lifetime. These characteristics give the triplet state a key role in many of the photochemical and photophysical processes involving fullerenes.[1] The magnetic properties of the lowest triplet state of fullerene derivatives were already investigated,[4,5] but important properties related to the triplet wave function, such as the orientation of the **g** and zero field splitting (**ZFS**) tensors in the molecular structure, are still unknown. The knowledge of the ZFS principal directions would help in designing efficient photoactive donor−acceptor systems containing fullerenes. In fact, the mutual orientation of the **ZFS** tensors of the donor−acceptor moieties plays a role in the triplet energy transfer process and therefore can influence the de-excitation pathway.[6,7]

In this article, we report on the full determination of the **g** and **ZFS** tensors of the excited triplet state of methanofullerene derivatives bearing substituents R═C(COOEt)$_2$. We investigated the C_{60} monoadduct (**mono)** shown in Scheme 1, and three bisadducts (**e**, **t3**, **t4**) with a second substituent in the highlighted positions. Due to the small **g** tensor anisotropy, high field EPR spectroscopy is required to determine the g principal values,[5] while the principal values of the **ZFS** tensor can be easily obtained from powder EPR spectra at the X band.[4] On the other hand, the orientation of the principal axes of magnetic tensors in the molecule requires the study of doped single crystals, normally difficult to obtain. The use of uniaxial media, such as nematic liquid crystals, was suggested,[8,9] but the low resolution of X-band EPR spectra and the lack of knowledge of the molecular orientation in the anisotropic medium prevented the assignment of the principal directions to the molecular structure.[8]

SCHEME 1

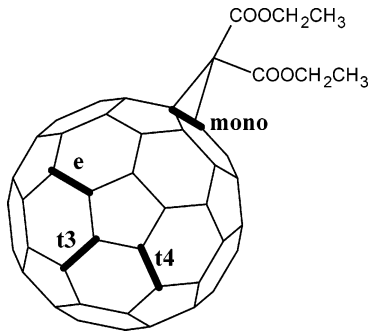

We show here that the **g** and **ZFS** tensors can be fully determined by combining (1) high-frequency TREPR experiments in a frozen nematic liquid crystal; (2) line shape analysis with a proper account of the anisotropic molecular distribution; (3) theoretical predictions of the molecular order in the nematic phase. The use of EPR at very high frequency with its increased **g** tensor resolution, and spectral simulations based on a biaxial distribution of the probe (three axes with different alignment tendency can be identified in the molecule) are essential for determining the orientation of the **ZFS** and **g** tensor axes with respect to the nematic C_∞ axis (director).[10] Finally, the principal axes in the molecular skeleton are assigned by relating the EPR results with theoretical predictions of molecular order.

Experimental Section

The synthesis of the studied compounds has been previously reported.[11] The liquid crystal E7 (Merck) was used as solvent. It has positive magnetic anisotropy $\Delta\chi$ and presents the solid-(263 K)-nematic-(333 K)-isotropic phase transitions. The samples were prepared by evaporating a fullerene solution in $CHCl_3$ contained in the quartz sample tube and subsequently redissolving the fullerenes in the nematic solvent. All solutions were deoxygenated using several freeze−pump−thaw cycles and then sealed under vacuum. The nematic solutions were oriented at room temperature in the 8.6 T magnetic field of the spectrometer and subsequently frozen at a temperature of 100 K. This allows recording spectra with the director axis parallel to the external

* To whom correspondence should be addressed: Fax:+39-049-8275239; E-mail:annalisa.maniero@unipd.it.
† Università di Padova.
‡ Florida State University.

10.1021/jp056223z CCC: $33.50
Published on Web 01/31/2006

magnetic field. The spectra for the field direction perpendicular to the director axis were obtained by rotating over 90° the frozen sample inside the spectrometer. The spectra were recorded using a unique multi-frequency super heterodyne quasi-optical spectrometer designed to operate at 120, 240, and 360 GHz.[12] The experiments described here were performed at 240 GHz without microwave cavity and using a relatively large sample volume (~100 μL). The optical excitation was obtained by a doubled Q-switched Nd:YAG laser (Continuum Powerlite), using pulses of 6 ns at 532 nm; the estimated energy at the sample corresponds to 5−10 mJ/pulse. A digital oscilloscope (HP Infinium) acquires the time evolution of the signal at each value of the magnetic field after the trigger from the laser, with one or two points being collected before the laser flash to allow a successive subtraction of time- and laser-independent background noise. Here we report the spectra taken immediately after the laser flash (integration window 0−3 μs) when the signal is maximum and has not started to decay yet. The signal decay can be fitted with a single exponential: at 100 K the signal decay time is 25 ± 5 μs for all the adducts and is rather homogeneous throughout the spectrum.

The field calibration has been done through an internal standard: a fragment of bis-diphenylene-phenylallyl (BDPA) in polystyrene, $g = 2.00261(2)$, has been added in the sample holder. Its field-modulated cw-spectrum has been recorded together with the TR-EPR spectrum of the excited fullerenes.

Theoretical Basis

The possibilility of fully determining the orientation of the **ZFS** tensor of a solute from triplet EPR spectra recorded in liquid crystals relies on the presence of three molecular axes with different propensity to align to the mesophase director. This is a general feature of molecules with relatively low symmetry, which do not possess, for instance, a C_n symmetry axis with $n \geq 3$.[13] The probability of the solute to have an orientation defined by the three Euler angles $\Omega = (\alpha,\beta,\gamma)$ in a frame with the Z axis parallel to the nematic director, is described by the single-particle distribution function:

$$p(\Omega) = Q^{-1} \exp[-U(\Omega)/k_B T] \quad (1)$$

where $U(\Omega)$ is the orientational mean field experienced by the solute and Q is the orientational partition function

$$Q = \int \exp[-U(\Omega)/k_B T]\, d\Omega \quad (2)$$

Using a generalized Maier−Saupe form,[14] in a molecular frame coincident with the principal ordering frame, the orienting mean field can be expressed as

$$U(\Omega)/k_B T = -\epsilon\{D^2_{00} + \lambda[D^2_{02}(\Omega) + D^2_{0-2}]\} \quad (3)$$

where $D^2_{0m}(\Omega)$ are Wigner rotation matrices.[15] The parameters ϵ and λ depend on the solute, and the magnitude of ϵ is related to the degree of order in the nematic medium, while λ represents the biaxiality of the orienting potential.

The alignment behavior of solutes in nematics is commonly described in terms of the Saupe matrix **S**,[16] which is completely defined by the ϵ and λ parameters. Its elements are defined as

$$S_{ij} = \frac{\langle 3 \cos \vartheta_{iZ} \cos \vartheta_{jZ} - \delta_{ij} \rangle}{2} \quad (4)$$

where ϑ_{iZ} is the angle between the ith molecular axis and the nematic director and the brackets denote the average over the orientational distribution eq 1. The diagonal S_{ii} components give the degree of order of the molecular axes. From the definition it follows that $-0.5 \leq S_{ii} \leq 1$, and $\sum_i S_{ii} = 0$. All S_{ii} values vanish in isotropic phase; the sign of S_{ii} identifies whether the ith molecular axis tends to lie parallel (> 0) or perpendicular (<0) to the nematic director. Molecules possessing a C_n symmetry axis with $n \geq 3$ are said to have a uniaxial orientational behavior, since the two components of the Saupe matrix perpendicular to C_n axis are identical.

SCHEME 2

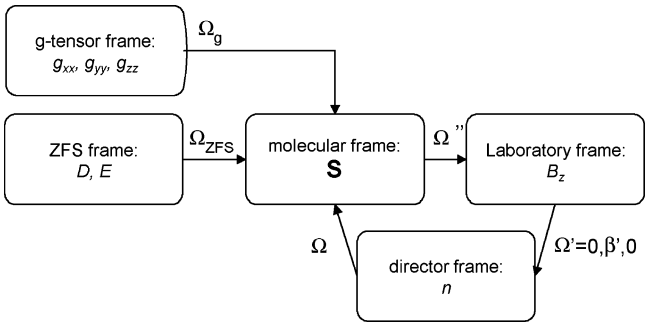

In this work, the Saupe matrices of the fullerene derivatives have been obtained in two ways: (i) from spectral simulations we obtained the $\mathbf{S}^{ZFS}$ matrix expressed in the principal frame of the **ZFS** tensor and (ii) from theoretical predictions we obtained the diagonal $\mathbf{S}^{Mol}$ matrix, in the principal ordering frame. For a given solute, the orientation of the principal axes of the **ZFS** tensor in the molecular structure is inferred from the comparison of the $\mathbf{S}^{ZFS}$ and $\mathbf{S}^{Mol}$ matrices.

(i) Spectral Simulations. Spectral simulations were performed with a model accounting for the partial order assumed by the solute in the nematic phase. Different reference frames have to be considered: (1) the **ZFS** and (2) the **g** tensor principal frames, which in principle are distinct; (3) the molecular reference frame (a,b,c), defined as the principal ordering frame of the molecule; (4) the laboratory frame defined by the external magnetic field aligned along the Z_{lab} axis; (5) the director frame, where the director n identifies the Z axis. Scheme 2 summarizes the transformations between these different reference frames.

The following spin Hamiltonian was considered:

$$H = \mu_B \mathbf{S}\cdot\mathbf{g}\cdot\mathbf{B} + \mathbf{S}\cdot\mathbf{D}\cdot\mathbf{S}$$

where the two terms are the electron−Zeeman and the electron−electron dipolar interactions, respectively. In this expression, μ_B is the Bohr magneton, **S** the total spin operator, **g** the g tensor, **B** the external magnetic field, and **D** the spin−spin dipolar tensor, with X, Y, and Z principal values ($Z>X>Y$). The diagonalization of the spin Hamiltonian gives the energies of the three triplet sublevels, corresponding in the high field approximation to $M_s = 1, 0, -1$ states, and the resonance fields (B_{res}) relative to the two allowed transitions $|-1\rangle \rightarrow |0\rangle$ (B_{res-}) and $|0\rangle \rightarrow |1\rangle$ (B_{res+}). The intensity of each transition depends on the nonequilibrium population difference ($P_\pm$) between the two states. Each triplet sublevel is a field-dependent linear combination of the zero-field states. Its population, determined by the selective intersystem crossing process from the excited singlet, is expressed by a linear combination of the zero-field populations.[17] Since the resonance field B_{res} and intensity of each transition depend on the molecular orientation Ω'' with respect to the laboratory frame (see Scheme 2), the spectral

intensity at each field value is calculated as the integral over the Euler angles Ω'':

$$I(B) = \sum_{\pm} \int G(B_{res\pm}(\Omega'') - B)\, P_{\pm}(\Omega'',B)\, p(\Omega'')\, d\Omega'' \quad (5)$$

The summation is over the two possible EPR transitions, $G(\Omega'')$ is the line shape function that was taken as Lorentzian and $P_{\pm}(\Omega'',B)$ is the nonequilibrium population difference between the upper and the lower level of the considered transition. The anisotropic molecular distribution, occurring in the partially ordered phase of the frozen liquid crystal, is introduced by the distribution function $p(\Omega'')$. It represents the probability of the solutes to be at a certain orientation Ω'' with respect to the magnetic field and can be easily obtained from eqs 1−3, by taking into account a further rotation Ω' from the laboratory to the director frame.

In general, the fitting parameters in the spectral simulation are: the principal values of the **ZFS** and **g** tensors, the two sets of angles that specify the orientation of the principal **ZFS** and **g** tensor systems relative to the molecular system (Ω_{ZFS}, Ω_g), the population of the zero field sublevels, the intrinsic line width, and the values of the parameters ϵ and λ appearing in the mean field potential (eq 3). In the program, the angle β' between the magnetic field and the director n (see Scheme 2) has to be introduced, and it is either 0° or 90° for parallel or perpendicular mutual orientation, respectively.

(ii) Surface Tensor Model. Predictions of the Saupe orientation matrix **S** of the fullerene derivatives have been obtained according to the surface tensor model.[18−20] This is a phenomenological approach that derives from the observation that in a nematic phase elongated molecules preferentially orient with the long axis parallel to the director. Within this approach, the mean field eq 3 is parameterized on the basis of the anisometry of the molecular surface. This simple description is meant to account for the anisotropy of short-range intermolecular interactions, which are modulated by the molecular shape. Despite its simplicity, the method has been successfully used for different classes of compounds in the nematic phase of thermotropic liquid crystals.[21]

The orienting potential is expressed as

$$U(\Omega)/k_BT = -\xi\{T^{20}D^2_{00}(\Omega) + T^{22}[D^2_{02}(\Omega) + D^2_{0-2}(\Omega)]\}$$
$$= -\xi T^{20}\{D^2_{00}(\Omega) + \lambda[D^2_{02}(\Omega) + D^2_{0-2}(\Omega)]\} \quad (6)$$

where T^{20} and T^{22} are irreducible spherical components of the surface tensor **T** (in its principal axis system). The elements of tensor **T** describe the surface anisometry along different directions. The parameter ξ, which gives the orienting strength of the medium, can be related to the reduced temperature (T/T_{ni} where T_{ni} is the nematic−isotropic transition temperature) and the structure of the nematic solvent;[18,19] in our calculations it has been taken as a free parameter. Equation 6 has the same form as eq 3, with $\epsilon = \xi T^{20}$ and $\lambda = T^{22}/T^{20}$.

Given the molecular geometry, the molecular surface is defined as the surface drawn by the center of a bead rolling on the assembly of interlocking van der Waals spheres centered on the nuclei[22] and is approximated by a set of triangles, obtained with the algorithm developed by Sanner et al.[23]

Results and Discussion

The TREPR spectra recorded at 100 K with the magnetic field parallel and perpendicular to the frozen nematic director are reported in Figures 1 and 2 (continuous lines). The spectra

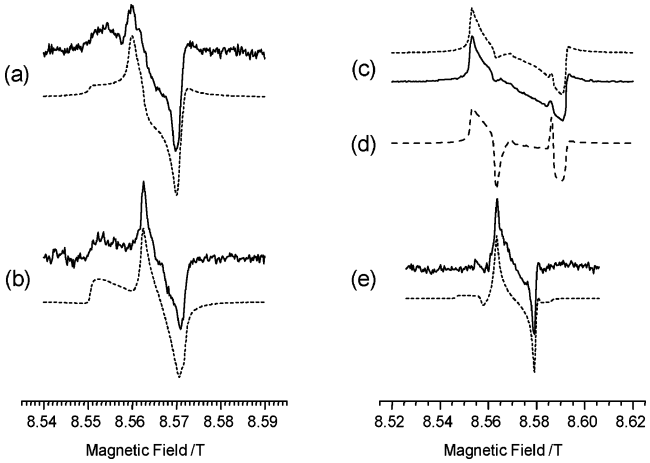

Figure 1. TR-EPR spectra (solid line) and simulations (dotted line) of the monoadduct (a,b) and the **e** bisadduct (c,e). Spectra obtained with the nematic director parallel (a,c), and perpendicular (b,e) to the external magnetic field. Trace (d) is the simulation of spectrum (c) obtained with a uniaxial distribution but parameters otherwise identical to those used for the best fitting simulation (dotted line).

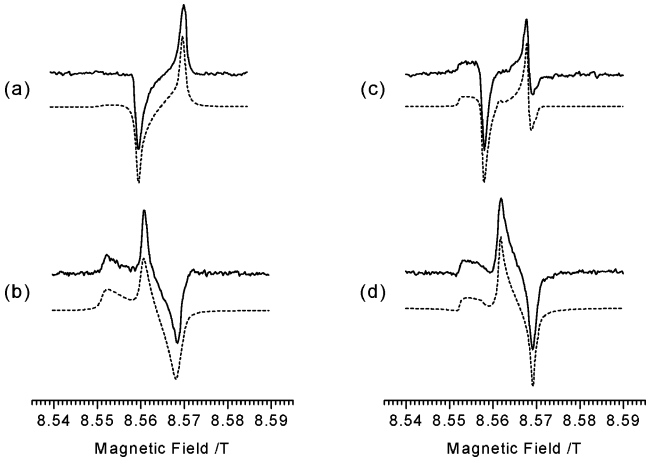

Figure 2. TR-EPR spectra (solid line) and simulations (dotted line) of the **t3** (a,b) and the **t4** (c,d) bisadducts. Spectra registered with the nematic director parallel (a,c) and perpendicular (b,d) to the external magnetic field.

show lines both in emission and enhanced absorption in a pattern that is consistent with a triplet state populated by intersystem crossing through spin−orbit coupling (SO−ISC). All features corresponding to the principal values of the **ZFS** tensor can be seen in TREPR spectra of isotropic samples. For the studied fullerene derivatives the pair of features, corresponding to each ZFS principal value, present the following absorption (A) − emission (E) pattern (from the largest to the smallest line splitting): A/E for the Z component, E/A for Y, and A/E for X.[5] The solute orientational order causes a marked deviation from the isotropic line shape, and some features may be absent in spectra obtained with the director parallel or perpendicular to the magnetic field (see, for example, the calculated spectra shown in the Supporting Information). The features appearing in each spectrum depend on the particular orientation assumed by the solute molecules with respect to the magnetic field, and of course on the orientation of the magnetic principal axes in the molecular frame. In the case of bisadducts, a degree of order higher than that of monoadduct can be direcly inferred from the marked difference between their spectra recorded with the magnetic field parallel and perpendicular to the nematic director.

Figures 1 and 2 also show simulated spectra (dotted lines) obtained as described in the Theoretical Basis section. For these

TABLE 1: Principal Values of the Saupe Matrix in the ZFS and in the Ordering Principal Frames[a]

	ZFS principal frame (spectral simulations)			Principal ordering frame (surface tensor calculations)		
adduct[b]	S_{XX}^{ZFS}	S_{YY}^{ZFS}	S_{ZZ}^{ZFS}	S_{aa}^{Mol}	S_{bb}^{Mol}	S_{cc}^{Mol}
mono	−0.26	0.52	−0.26	−0.26	−0.26	0.52
t3	−0.22	0.52	−0.30	−0.31	−0.21	0.52
t4	−0.30	0.39	−0.09	−0.30	−0.09	0.39
e	−0.29	0.00	0.29	−0.29	0.01	0.28

[a] For reference, the ZFS (/MHz) and the **g** tensor principal values are reported from ref 5. [b] **mono:** X = −89, Y = −102, Z = 191; g_{xx} = 2.00065, g_{yy} = 2.00115, g_{zz} = 2.00215. **t3:** X = −75, Y = −98, Z = 173; g_{xx} = 2.00121, g_{yy} = 2.00115, g_{zz} = 2.00213. **t4:** X = −72, Y = −97, Z = 169; g_{xx} = 2.00121, g_{yy} = 2.00182, g_{zz} = 2.00219. **e:** X = −145, Y = −224, Z = 369; g_{xx} = 2.00116, g_{yy} = 2.00171, g_{zz} = 2.00226.

simulations the principal values of the **g** and **ZFS** tensors and populations of triplet sublevels were taken identical to those determined for the adducts in glassy toluene.[5] This assumption was confirmed using the same parameters to simulate the spectra recorded in nematic solution frozen at zero field, i.e., with isotropic molecular distribution (data not shown). The best fitting of the spectra provided the Saupe matrix defining the orientational distribution of the **ZFS** and **g** tensor axes ($\mathbf{S}^{ZFS}$), together with the two set of angles specifying the orientation of the ZFS and **g** tensor principal frames with respect to the molecular order axes (*a*,*b*,*c* system). The **ZFS** and **g** tensors resulted to be diagonal in the same frame (within ±15°, determined by the line shape sensitivity to the mutual orientation of the magnetic tensors); therefore, all results relative to the **ZFS** tensor apply to the **g** tensor as well. The error estimate on the $\mathbf{S}^{ZFS}$ elements is of the order of ±0.01 and is based on the line shape sensitivity to ϵ and λ.

For a given sample, simultaneous fit of the spectra obtained with the magnetic field parallel and perpendicular to the nematic director was performed. Figures 1 and 2 show excellent agreement between experimental and simulated spectra. For the sake of comparison, the line shape obtained under the assumption of uniaxial orientation of the **e** bisadduct is shown in Figure 1d; its inadequacy to simulate the 240 GHz spectrum clearly appears. In the past, X band spectra of organic solutes of various symmetries were interpreted by assuming uniaxial behavior.[8] Biaxial alignment, along with the sensitivity of the high field experiments to this feature are necessary requirements for the complete assignment of the magnetic tensors. The Saupe matrices $\mathbf{S}^{ZFS}$ obtained from the best fit simulations are reported in the first three columns of Table 1. The presence of substituents that modify the high C_{60} symmetry leads to sizable order parameters. Moreover, the results clearly show that the adduct substitution pattern drives the molecular alignment. At variance to the monoadduct, all the bisadducts exhibit a nonnegligible biaxiality of the order of the ZFS principal axes ($S_{XX}^{ZFS} \neq S_{YY}^{ZFS} \neq S_{ZZ}^{ZFS}$).

While the spectral simulations give the orientation of the ZFS axes with respect to the nematic director, for identifying these directions in the molecular skeleton, the EPR data were related to predictions of the orientational order in the nematic, based on the surface tensor method described in the Theoretical Basis section. The structure of the C_{60} derivatives that is required to generate the molecular surface was obtained by geometry optimization (in the ground state) with the semiempirical PM3 method.[24] In general, several conformers are possible; only one was considered, following the criteria of the highest symmetry and lowest energy. In constructing the molecular surfaces,

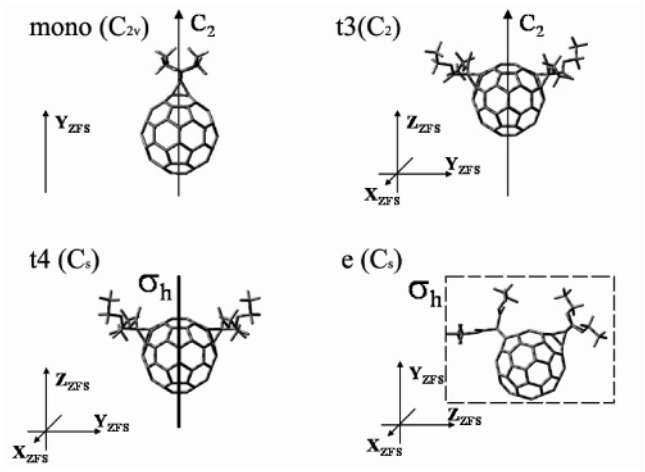

Figure 3. The investigated C_{60} fullerene derivatives with the orientation of the ZFS axes obtained in this work (for bisadducts the X_{ZFS} axis is perpendicular to the page). The **g** tensor principal axes are parallel to the ZFS axes. The symmetry point group of the adducts is reported as well as the principal symmetry elements.

hydrogen atoms were neglected and for the other atoms the following radii were assumed: r_C = 1.85 Å, r_O = 1.5 Å, along with a rolling sphere radius r_0 = 3 Å.

The principal values of the Saupe matrix obtained from calculations are reported in the last three columns of Table 1. Labels of the principal alignment axes are assigned to be $S_{cc}^{Mol} > S_{bb}^{Mol} > S_{aa}^{Mol}$. We can see that, apart from the different labeling, the two Saupe matrices, obtained for a given derivative from spectra simulation and calculations, are practically identical. Comparison of the two parts of Table 1 allows us to locate the ZFS axes on the molecule. The results are summarized in Figure 3. In the case of monoadduct, the small shape biaxiality introduced by the substituent is not sufficient to produce a difference in the alignment perpendicular to the C_2 symmetry axis. As a consequence, full assignment of the ZFS axes is not possible, and only the Y principal direction, which is parallel to the C_2 axis, can be determined. For the bisadducts the X principal axis is perpendicular to [6−6] bonds, while the orientation of the other ZFS axes depends on the substitution pattern. A clear difference can be observed between **t3** and **t4** on one side, and **e** on the other.

The very good accord between results obtained from the spectral simulations and surface tensor calculations gives a strong support to the reliability of the method we have used to determine the orientation of the **ZFS** and **g** tensor principal axes in the molecular frame. The method is quite general and can be used for the determination of the **ZFS** tensor of the excited triplet of molecules of arbitrary structure. Full assignment of the ZFS principal axes is possible, provided that the molecule has a biaxial orientational behavior in the nematic phase. We applied the method to the study of fullerene derivatives, finding that the ZFS parameters of the lowest triplet state are strongly dependent on the substituent pattern, without a recognizable general trend. This dependence reflects the different perturbing effect of substituents on the triplet electronic wave function of C_{60}. In some cases, e.g., for the equatorial bisadduct compared to the other bisadducts, this is associated with a significant change of the ZFS principal values.[5] However, the results obtained for mono and trans derivatives show that also similar values of the ZFS parameters can correspond to a very different electronic distribution, as inferred from the different orientation of the ZFS axes in the molecular skeleton. In conclusion, the information on the triplet wave function can hardly be trans-

ferred from one fullerene adduct to another, and the triplet features of the specific C_{60} derivative should be considered when dynamic processess involving photophysical properties of fullerenes are studied.

Acknowledgment. M.B. thanks the NHMFL and the National Science Foundation (CHE-9601731) for financial support.

Supporting Information Available: Effects of the biaxiality parameter λ on TREPR spectral line shape. This material is available free of charge via the Internet at http://pubs.acs.org.

References and Notes

(1) *Optical and electronic properties of fullerenes and fullerene-based materials*, Shinar, J., Vardeny, Z. L., Kafafi, Z. H., Eds.; Marcel Dekker: New York, 2000.

(2) Guldi, D. M.; Prato, M. *Acc. Chem Res.* **2000**, *33*, 695.

(3) Gust, D.; Moore, T. A.; Moore, A. L. *Acc. Chem. Res.* **2001**, *34*, 40.

(4) Pasimeni, L.; Hirsch, A.; Lamparth, I.; Herzog, A.; Maggini, M.; Prato, M.; Corvaja, C.; Scorrano, G. *J. Am. Chem. Soc.* **1997**, *119*, 12896.

(5) Bortolus, M.; Prato, M.; van Tol, J.; Maniero, A. L. *Chem. Phys. Lett*. **2004**, *398*, 228.

(6) Regev, A.; Galili, T.; Levanon, H. *J. Phys. Chem*. **1996**, *100*, 18502.

(7) Galili, T.; Regev, A.; Levanon, H.; Schuster, D. I.; Guldi, D. M. *J. Phys. Chem. A* **2004**, *108*, 10632.

(8) Pasimeni, L.; Segre, U.; Ruzzi, M.; Maggini, M.; Prato, M.; Kordatos, K. *J. Phys. Chem. B* **1999**, *103*, 11275.

(9) Ceola, S.; Corvaja, C.; Franco, L. *Mol. Cryst. Liq. Cryst*. **2003**, *394*, 31.

(10) Shuali, Z.; Berg, A.; Levanon, H.; Vogel, E.; Broring, M.; Sessler, J. L. *Chem. Phys. Lett.* **1999**, *300*, 687.

(11) Hirsh, A.; Lamparth, I.; Karfunkel, H. R. *Angew. Chem., Int. Ed. Engl.* **1994**, *33*, 437.

(12) van Tol, J.; Brunel, L. C.; Wylde, R. J. *Rev. Sci. Instrum.* **2005**, *76*, 074101.

(13) Zannoni, C. In *The Molecular Physics of Liquid Crystals*; Luckhurst, G. R., Gray, G. W., Eds.; Academic Press: London, 1979.

(14) Luckhurst, G. R. In *The Molecular Physics of Liquid Crystals*; Luckhurst, G. R., Gray, G. W., Eds.; Academic Press: London, 1979.

(15) Zare, N. R. *Angular Momentum*; Wiley: New York, 1987.

(16) Vertogen, G.; de Jeu, W. H. *The Physics of Liquid Crystals, Fundamentals*, Springer: Berlin, 1988.

(17) McGlynn, S. P.; Azumi, T.; Kinoshita, M. *Molecular Spectroscopy of the Triplet State*; Prentice Hall: Engelwood Cliffs, NJ, 1969.

(18) Ferrarini, A.; Moro, G. J.; Nordio, P. L.; Luckhurst, G. R. *Mol. Phys.* **1992**, *77*, 1.

(19) Ferrarini, A.; Janssen, F.; Moro, G. J.; Nordio P. L. *Liq. Cryst.* **1999**, *26*, 201.

(20) Ferrarini, A.; Moro, G. J. In *NMR of Ordered Liquids*; Burnell, E. E., de Lange, C. A., Eds.; Kluwer: Amsterdam, 2003.

(21) Ferrarini, A.; Moro, G. J.; Nordio, P. L. In *Physical Properties of Liquid Crystals*, (*EMIS Datareviews Series*); Dunmur, D. A.; Fukuda, A.; Luckhurst, G. R., Eds.; IEE: London, 2000.

(22) (a) Richards, F. M. *Annu. Rev. Biophys. Bioeng.* **1977**, *151*, 6. (b) Connolly, M. J. *J. Appl. Crystallogr*. **1983**, *16*, 584.

(23) Sanner, M. F.; Spehner, J.-C.; Olson, A. *Biopolymers* **1996**, *38*, 305.

(24) Frisch, M. J.; Trucks, G. W.; Schlegel, H. B.; Scuseria, G. E.; Robb, M. A.; Cheeseman, J. R.; Zakrzewski, V. G.; Montgomery, J. A., Jr.; Stratmann, R. E.; Burant, J. C.; Dapprich, S.; Millam, J. M.; Daniels, A. D.; Kudin, K. N.; Strain, M. C.; Farkas, O.; Tomasi, J.; Barone, V.; Cossi, M.; Cammi, R.; Mennucci, B.; Pomelli, C.; Adamo, C.; Clifford, S.; Ochterski, J.; Petersson, G. A.; Ayala, P. Y.; Cui, Q.; Morokuma, K.; Malick, D. K.; Rabuck, A. D.; Raghavachari, K.; Foresman, J. B.; Cioslowski, J.; Ortiz, J. V.; Stefanov, B. B.; Liu, G.; Liashenko, A.; Piskorz, P.; Komaromi, I.; Gomperts, R.; Martin, R. L.; Fox, D. J.; Keith, T.; Al-Laham, M. A.; Peng, C. Y.; Nanayakkara, A.; Gonzalez, C.; Challacombe, M.; Gill, P. M. W.; Johnson, B. G.; Chen, W.; Wong, M. W.; Andres, J. L.; Head-Gordon, M.; Replogle, E. S.; Pople, J. A. *Gaussian 98*, Gaussian, Inc.: Pittsburgh, PA, 1998.